Observing the non-analytic behaviour of a qubit-resonator system

Gleb Fedorov[1,2], Evgenii Glushkov[1,2] and Kirill Shulga[1,2,3]

[1]*Moscow Institute of Physics and Technology* [2]*Moscow Institute of Steel and Alloys* [3]*Russian Quantum Center*

Introduction

The performance of superconducting qubits has improved by several orders of magnitude in the past decade. Some of the most successful and prominent studies [1] in this field are about circuit Quantum Electrodynamics (cQED) or so-called “quantum optics on a chip”. In this work we’ve been trying to test if our sample was robust enough to reproduce quantitatively famous effects predicted by so-called “Rabi model”.

Flux qubit

In our experiment the Flux qubit was used. Firstly suggested in 1999, this qubit consists of a superconducting loop, interrupted with three Josephson junctions as depicted on Fig. 1 (a), (b).

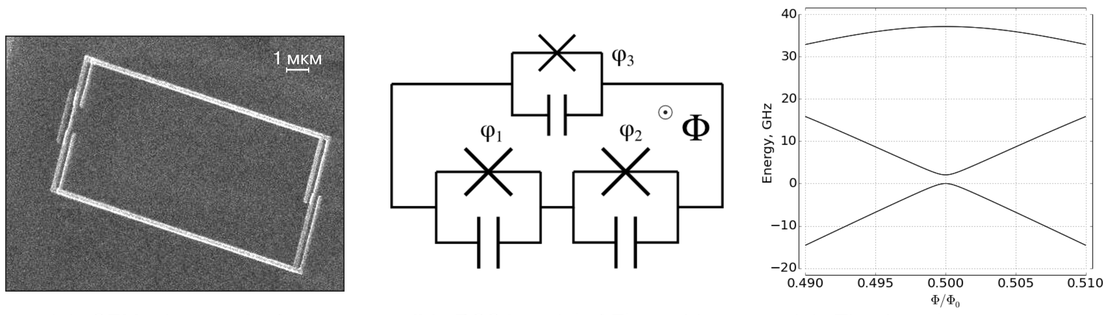

(a): SEM micrograph of a three-junction Flux qubit

(b): RCSJ model of Flux qubit

(c): The three lowest energy bands

Fig. 1: Flux qubit, its theoretical model and numerically computed energy spectrum

RCSJ model of the Josephson junction and the quantization of flux allows to write down the Hamiltonian of the Flux qubit and to solve it for eigenenergies and eigenstates. The first three of numerically calculated energy levels are presented on Fig. 1 (c). The difference $E_1 - E_0$ shows a hyperbolic dependence on Φ (Fig. 2).

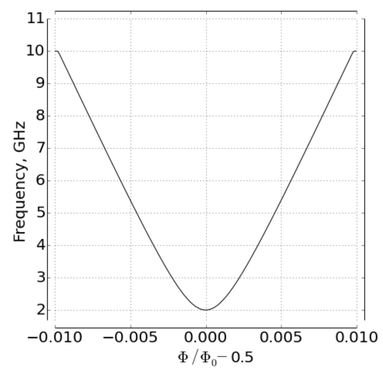

Fig. 2: Flux qubit spectrum

In the vicinity of the degeneracy point $\Phi = \Phi_0/2$ one can describe the qubit with a reduced two-level Hamiltonian:

$$\hat{\mathcal{H}} = \frac{\varepsilon}{2}\hat{\sigma}_z + \frac{\Delta}{2}\hat{\sigma}_x, \tag{1}$$

where $\varepsilon \propto \Phi - \Phi_0/2$ and $\Delta = const$ is responsible for the minimal splitting. From this we get the theoretical formula for the numerically obtained spectrum on Fig. 2:

$$\Delta E = \hbar\omega_q = \sqrt{\varepsilon^2 + \delta^2}. \tag{2}$$

Sample design

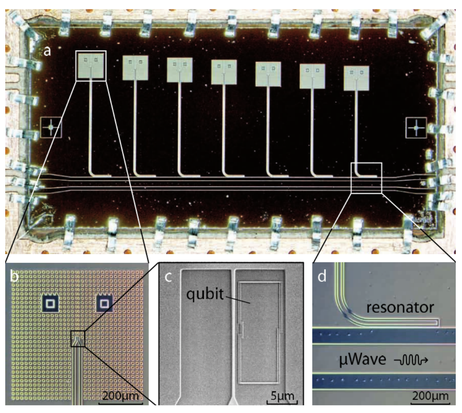

Fig. 3: Seven qubit-resonator systems coupled to the transmission line

We used a chip with seven $\lambda/4$ microwave resonators with different consequent resonance frequencies around 10.7 GHz, each with a Flux qubit at the end. They were capacitively coupled to the transmission line and are experimentally recognized by a significant drop of S_{21} when the signal is on the resonance. The qubits can be detected via scanning through a range of currents in a superconducting coil surrounding the chip. All the data presented here corresponds to the 5th resonator.

Two-tone spectroscopy

To obtain the qubit part of the compound spectrum on Fig. 5 (a) a second tone driving can be added using a coupler or a fast bias coil. This method is conceptually close to the dispersive readout. When the second tone is in resonance with the qubit it induces damped Rabi oscillations in it thus reducing the steady-state transition amplitude for the first tone. Consequently, the absorption is reduced. The experimental results are presented on Fig. 4. As one can see, the linewidth of the spectrum is huge (≈1 GHz), implying significant dissipation.

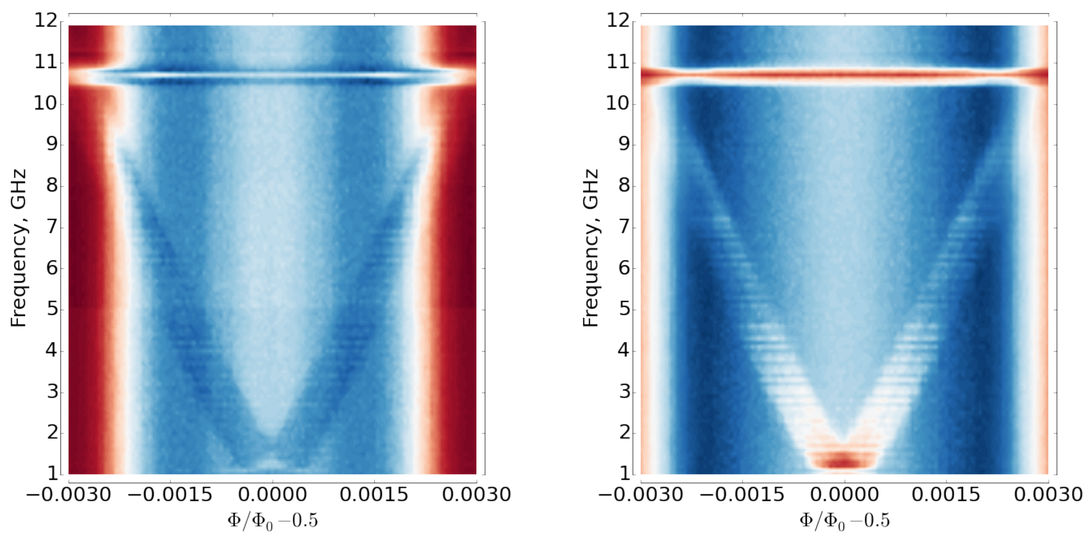

(a): $20\log|S_{21}|$ plot

(b): Arg $[S_{21}]$ plot

Fig. 4: Two tone spectra

Rabi model

The theoretical model describing the interaction of the qubit includes unitary dynamics governed by Rabi Hamiltonian, three channels of dissipation, microwave driving of resonator. The voltage drop is taken to be proportional to $|\langle\hat{a}\rangle|$ in the steady-state, where $\hat{a}$ is the resonator annihilation operator. The master equation to determine the latter follows:

$$\begin{aligned}\hat{\mathcal{H}}_R = \frac{\hbar\omega_q}{2}\hat{\sigma}_z + \hbar\omega_r\left(\frac{1}{2} + \hat{a}^\dagger\hat{a}\right) + \hbar g(\hat{a}^\dagger + \hat{a}) \otimes (\hat{\sigma}_x \sin\theta - \hat{\sigma}_z\cos\theta) + \\ + A\cos(\omega t)(\hat{a}^\dagger + \hat{a}) + \kappa\mathcal{D}[\hat{a}] + \gamma\mathcal{D}[\hat{\sigma}^-] + \gamma_\phi\mathcal{D}[\hat{\sigma}_z],\end{aligned} \tag{3}$$

where $\tan\theta = \frac{\Delta}{\varepsilon}$ and (1) and (2) were used to make a correct basis transformation. The spectrum one can obtain from this model including only ω_{01} and ω_{02} frequencies is shown on Fig. 5.

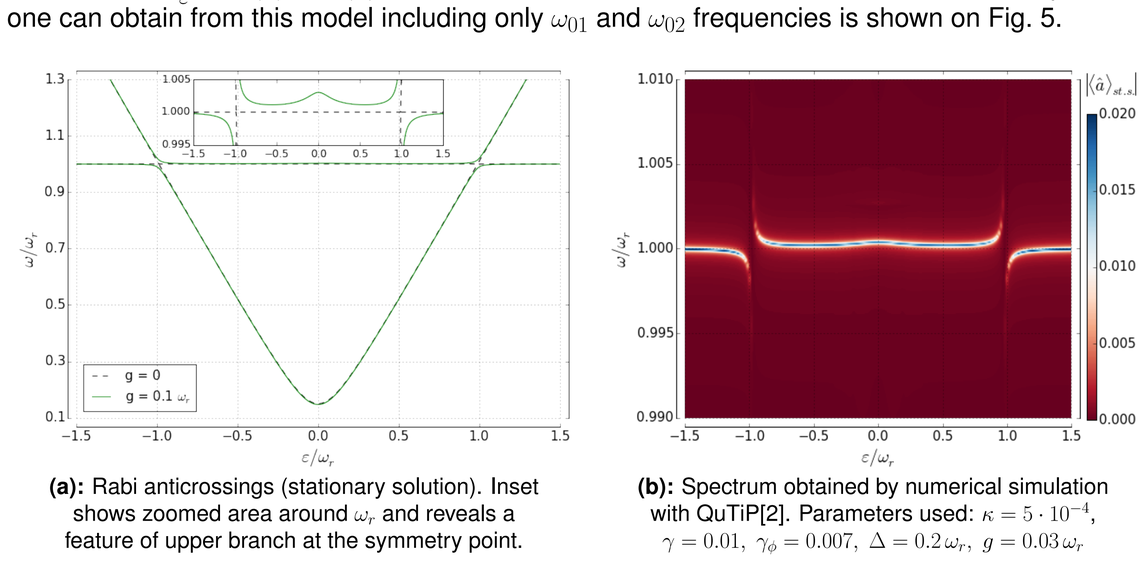

(a): Rabi anticrossings (stationary solution). Inset shows zoomed area around ω_r and reveals a feature of upper branch at the symmetry point.

(b): Spectrum obtained by numerical simulation with QuTiP[2]. Parameters used: $\kappa = 5\cdot10^{-4}$, $\gamma = 0.01,\ \gamma_\phi = 0.007,\ \Delta = 0.2\,\omega_r,\ g = 0.03\,\omega_r$

Fig. 5: The static and dynamic spectra of Rabi Hamitlonian.

It can be seen on Fig. 5 (a) that at the degeneracy point both frequencies have stronger deviations from unperturbed spectrum than in the other areas of dispersive regime. That happens due to the effective dependence of coupling constant $g_{eff} = g\sin\theta$ on flux bias.

Fig. 5 (b) shows how the system will react to driving with $A(\hat{a}^\dagger + \hat{a})\cos\omega t$. The part of the spectrum around ω_r will only be observed – qubit flips are suppressed for this operator, so there is no absorption at the bare qubit frequency ω_q.

Anticrossings

The main idea of this study was to compare the prediction of model (3) with the experimentally obtained spectrum. On Fig. 6 the two outcomes are shown, theoretical (a) and experimental (b). The fitting parameters were the coupling constant, flux-axis scale, unknown bare resonator frequency and three dissipation rates. Although it is one of the best possible fits, there are significant differences between plots in the upper branch.

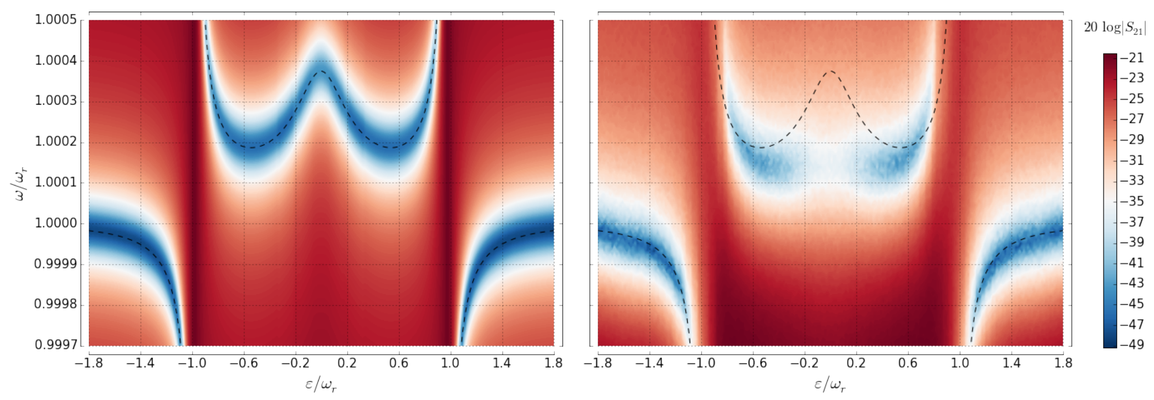

(a): Theoretical plot (z-scale normalized). Parameters same as in Fig. 5 (b) except for increased $\kappa = 6.5\cdot10^{-4}$. Plot follows the dashed line.

(b): Experimental plot. The middle peak is absent and the upper branch is too low and too narrow. Lower branch matches.

Fig. 6: Theoretical vs. experimental data for anticrossings. The dashed line shows the prediction of stationary Schrödinger equation to simplify comparison.

Another effect that was investigated was the “vanishing of anticrossings”. That means the impossibility to observe Rabi splitting of absorption peak in resonant regime. In the limit of “bad” qubit (lifetimes up to 1000 times shorter than of the photon inside the resonator) it was possible to model this effect theoretically (qualitatively) - indeed, peaks fade out before entering the anticrossing area, see Fig. 7 and additionally Fig. 5 (b).

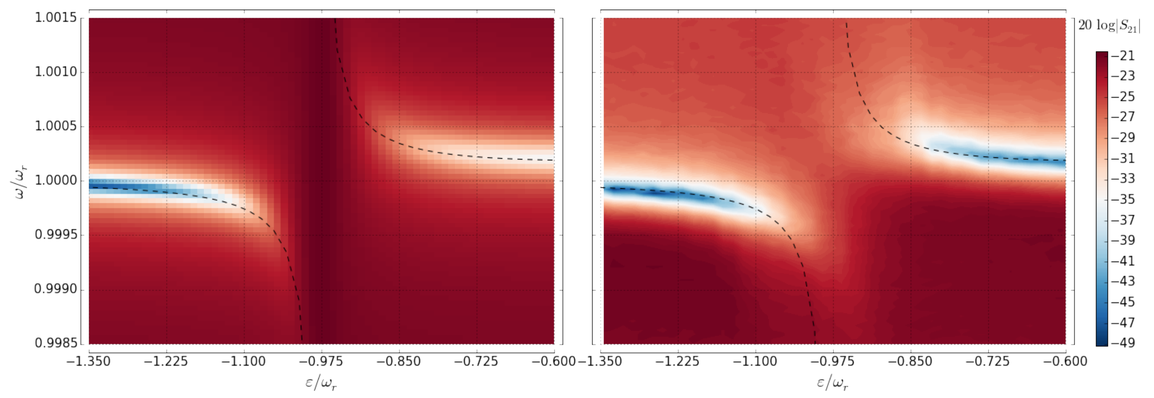

(a): Theoretical plot (z-scale normalized). Parameters same as in Fig. 6 (a) except for $\gamma = \gamma_\phi = 0.1$. Plot still follows the dashed line.

(b): Experimental plot. It can be seen that the right branch is much brighter than theory predicts and is too high above the dashed line.

Fig. 7: Theoretical vs. experimental data for anticrossing vanishing. The dashed line shows the prediction of stationary Schrödinger equation to simplify comparison.

Conclusion

The experiment we have conducted has shown that the our qubit-resonator system can’t be described by Rabi model. This result probably has its roots in the sample defects, which are hard to model. Nevertheless, qualitative effects are observable even with a qubit of low quality.

References

[1] Lev S Bishop, JM Chow, Jens Koch, AA Houck, MH Devoret, E Thuneberg, SM Girvin, and RJ Schoelkopf. Nonlinear response of the vacuum rabi resonance. *Nature Physics*, 5(2):105–109, 2009.

[2] J. R. Johansson, P. D. Nation, and F. Nori. Qutip: An open-source python framework for the dynamics of open quantum systems. *Computer Physics Communications*, 183(8):1760–1772, 2012.